Molecular Origin of Selectivity Differences Between Pd and AuPd in Benzyl Alcohol Oxidation: Different Oxygen Adsorption Properties

Aditya Savara,*[a] Carine E. Chan-Thaw,[b] Jonathan E. Sutton,[a] Di Wang,[c] Laura Prati,[b] and Alberto Villa*[b]

Abstract: The same mechanism and microkinetic model used for benzyl alcohol oxidation over Pd/C is shown to apply to benzyl alcohol oxidation over AuPd/C. Almost all of the selectivity differences are explained by a decrease in oxygen adsorption on AuPd. After isolating oxygen adsorption as being the origin of the selectivity differences, density functional theory was used to investigate the oxygen adsorption properties of a pure Pd surface, a pure Au surface, and an alloyed AuPd surface. These calculations show that Au-Pd alloying decreases the oxygen adsorption properties relative to pure Pd, explaining the selectivity differences, consistent with the microkinetic modeling.

The oxidation of benzyl alcohol by supported noble metals has been the subject of growing interest.[1] The main oxidation product is benzaldehyde, an important intermediate in the fragrances and food industry.[2] Side-products, such as benzene, toluene, benzoic acid, benzyl benzoate, and benzyl ether, have also been observed.[2] Au and Pd nanoparticles are the most studied catalysts for this reaction:[1b,1c,3] Pd for its resistance to deactivation, and Au for its high activity.[3] Recently, attention has been devoted to Au-Pd for liquid phase oxidation of alcohols.[1c,4] One reason for this interest is the fact that Au and Pd can form solid solutions in the whole range of the Au/Pd atomic ratios, and the addition of the second metal can alter the electronic and geometrical properties with the formation of alloy and/or core-shell structures.[5] It has been shown that alloying Au to Pd catalysts modify the catalytic activity and selectivity.[5] For example, under specific reaction conditions, the addition of Au to Pd has been shown to limit the formation of toluene, which implies a hindering the disproportionation pathway.[3a,3c,3d] The chemical origins of these differences between AuPd and Pd selectivities in the benzyl alcohol oxidation has not been completely understood.

We previously used microkinetic modeling (simulation + fitting[6]) to validate and understand the mechanism for benzyl alcohol oxidation to various products (benzaldehyde, toluene, benzoic acid, ...) over Pd/C.[6a] Here, we apply the same microkinetic model based on the mechanism in Scheme 1 to understand the differences in benzyl alcohol oxidation over AuPd/C relative to Pd/C, and then use density functional theory calculations to validate the differences in oxygen adsorption properties inferred from the microkinetic modeling.

The same range of temperature and concentration conditions as the previous study were used (Table S1),[6a] and the same microkinetic model (Table S2). The AuPd/C catalyst was prepared following a two-step procedure to produce homogenous-alloyed AuPd nanoparticles.[5b] The total metal loading was 1%wt, with Au/Pd molar ratio of 6:4. Activated carbon X40S from Camel was used as support. The support did not show any activity in the benzyl alcohol oxidation under the selected reaction conditions. HRTEM images reveal that most of the AuPd particles are multiply twinned in the form of decahedra or truncated decahedra (Figure 1).[5b] The uniform lattice spacings between the Pd (111) plane (2.25 Å) and the Au (111) plane (2.35 Å), confirmed the alloy state (Figure 1).[7]

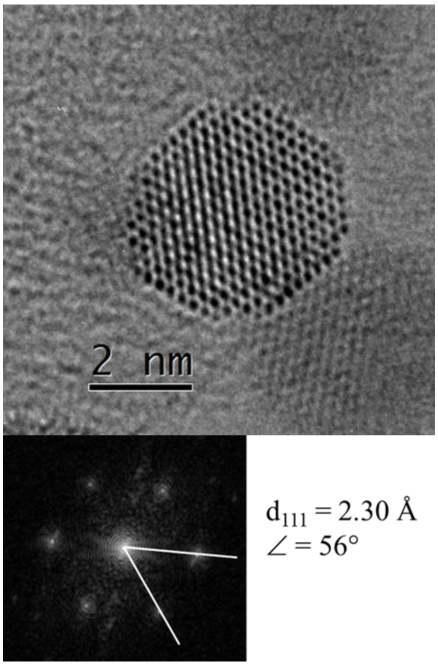

Figure 1. Representative HRTEM image of a multiply twinned particle in the form of truncated decahedron configuration with insets showing FFTs

---

[a] Dr. A. Savara, Dr. J. E. Sutton
Chemical Sciences Division
Oak Ridge National LaboratoryInstitution
1 Bethel Valley Road MS 6201, Oak Ridge, TN 37831
E-mail: savaraa@ornl.gov
[b] Dr. E.C. Chan-Thaw, Prof. L. Prati, Dr. A. Villa.
Dipartimento di Chimica
Università degli Studi di Milano
via Golgi 19, 20133, Milano, Italy
E-mail: alberto.villa@unimi.it
[c] Dr. D. Wang
Institute of Nanotechnology and Karlsruhe Nano Micro Facility,
Karlsruhe Institute of Technology, Hermann-von-Helmholtz-Platz 1,
D-76344 Eggenstein-Leopoldshafen, Germany

Supporting information for this article is given via a link at the end of the document.

Scheme 1. This scheme has been reproduced from Reference 6a with permission from Wiley-VCH.

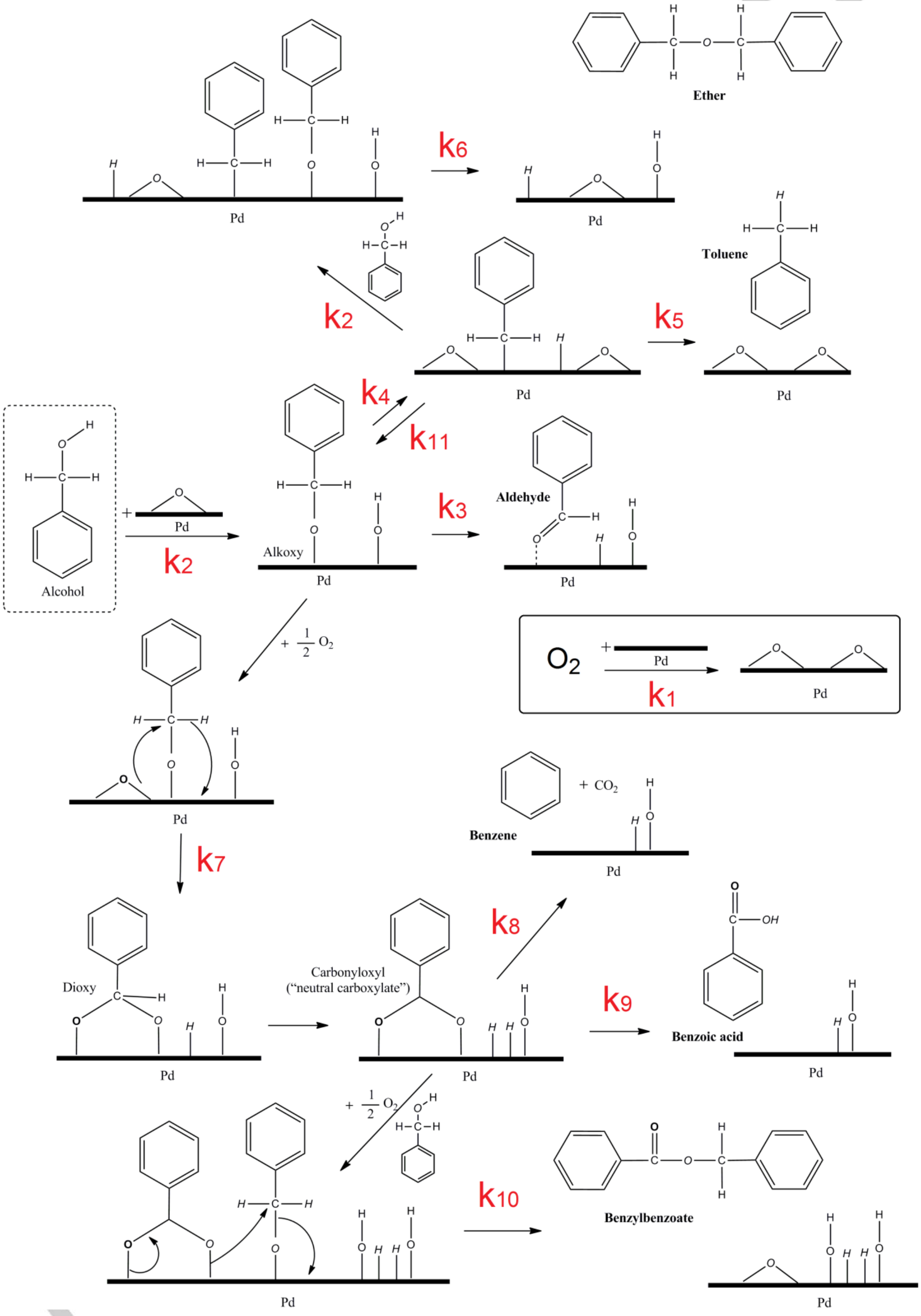

All data points here were measured at 60 minutes of reaction time, which was found to be suitable for microkinetic modelling of the AuPd/C data. First, we used microknetic modeling to reproduce the experimental data for the AuPd experiments at 70 °C. The previously obtained rate constant values for Pd/C were used as an initial guess followed by gradient optimization of the kinetic parameters (i.e., rate constants in Table 1).

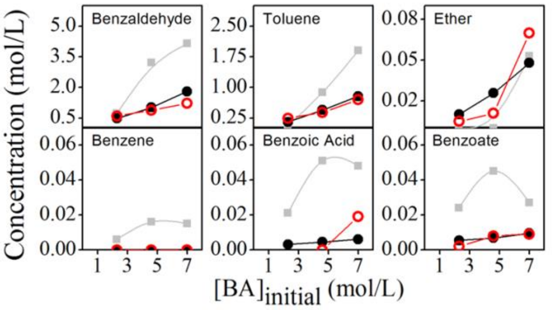

Figure 2: Trends for AuPd/C expressed as concentration of products vs initial concentration of benzyl alcohol (BA). Experimental points: open red circles, Microkinetic model: filled black circles. Experimental data points from Pd/C are shown in gray for comparison.

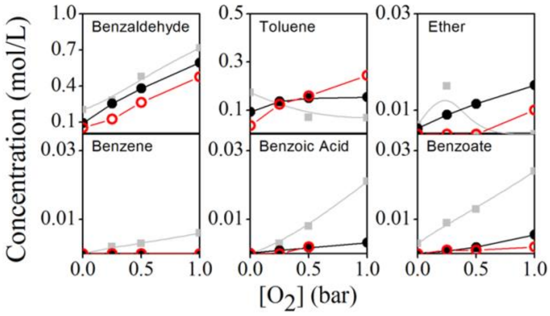

Figure 3: Trends for AuPd/C expressed as concentration of products vs oxygen pressure. Experimental data points from Pd/C are shown in gray for comparison.

Figures 2 and 3 show the results of this fitting: we see that the microkinetic model reproduced the trends for AuPd/C (red versus black circles). The selectivity for AuPd/C differs from that of Pd/C: experimental data points for Pd/C are shown in gray for comparison. Unlike the Pd/C data, the AuPd/C data is mostly monotonic. The simulations reproduce all of the trends over AuPd/C with mostly quantitative agreement, indicating agreement between the kinetic and mechanistic model with the experiments. The rate constants obtained from fitting are shown in Table 1, alongside the rate constants previously obtained for Pd/C. Under these conditions, AuPd/C has a lower activity compared to Pd/C and shows a different product distribution with less formation of products from the “carbonyloxyl” pathway (benzene, benzoic acid, benzoate) (Table 2).[3d] A different selectivity was obtained over Pd/TiO_2 and AuPd/TiO_2 (60°C, pO_2= 2 bar, toluene as solvent).[8] It appears clear that the support and the reaction conditions can affect the selectivity and mechanism of the alcohol oxidation over Pd versus AuPd. In this study, the carbon support is inactive for the reaction and enables us to compare the selectivity over the different particles directly.

Table 1: Fitted Rate Constants from Microkinetic Model at 70 °C. **

k	Value for Pd/C [From ref 6]	Value for AuPd/C [This study]
k1	8.2×10^{0} s^{-1} bar^{-1}	1.6×10^{0} s^{-1} bar^{-1}
k2	1.4×10^{-1} s^{-1} mol^{-1} L	1.6×10^{-1} s^{-1} bar^{-1}
k3	5.1×10^{6} s^{-1}	4.2×10^{6} s^{-1}
k4	6.7×10^{8} s^{-1}	6.2×10^{8} s^{-1}
k5	4.4×10^{14} s^{-1}	1.6×10^{14} s^{-1}
k6	2.9×10^{11} s^{-1}	6.1×10^{11} s^{-1}
k7	1.6×10^{6} s^{-1}	1.4×10^{6} s^{-1}
k8	1.4×10^{14} s^{-1}	1.6×10^{14} s^{-1}
k9	5.5×10^{14} s^{-1}	5.5×10^{14} s^{-1}
k10	9.4×10^{12} s^{-1}	5.4×10^{12} s^{-1}
k11	2.2×10^{11} s^{-1}	2.2×10^{11} s^{-1}

** For AuPd, the amount of benzene produced at 70 °C was too low to detect. The value provided for k8 at 70 °C was determined by gradient optimization during fitting of the temperature dependent data.

Table 2. Comparison of the activity and selectivities of Pd/C and AuPd/C[a]

Cat.	Selectivity (%)					
	Aldehyde	Toluene	Benzene	Acid	Ether	Benzoate
Pd/ AC	83	7.9	0.70	2.4	0	5.5
AuPd/ AC	65	33	0	0	1.3	0.54

[a] 25% benzyl alcohol / 75% xylene (vol/vol), 70°C, 1 Bar O_2 (flow 30 mL/min).

Table 3: Results of DFT calculations for the energies (kJ/mol) of adsorption and activation of O_2 on pure Pd and Au and the most stable of the AuPd alloys checked. Binding energies are with respect to clean slabs and gas-phase O_2. (A positive binding energy denotes a repulsive interaction between the molecule and the surface.)

Surface	O_2 (ads) Binding Energy	2O (ads) Binding Energy	Activation Energy
Pd	-90	-247	55
Au	6	-33	98
AuPd	5	-53	92

As shown in Figure 4, the differences between palladium and AuPd are almost entirely due to k1: Figure 4 shows the ratios of the logs of the rate constants for AuPd/C vs. Pd/C, where the largest change (by far) on this log scale was in k1. Nearly all of the selectivity changes can be explained by this change in k1, which corresponds to oxygen adsorption. This finding makes sense in the context of our mechanistic studies: the aldehyde route and the carbonyloxyl pathways *both* require surface oxygen, while the Toluene route is facilitated by a lack of surface oxygen. Figure 5 shows this selectivity difference, and also shows that increasing the oxygen pressure has less of an effect over AuPd relative to over Pd. To strengthen this point and validate the idea that oxygen adsorption would be different on the AuPd surface versus the Pd surface, DFT calculations on the strength and activation energies of oxygen adsorption on Pd and AuPd were performed (Table 3).

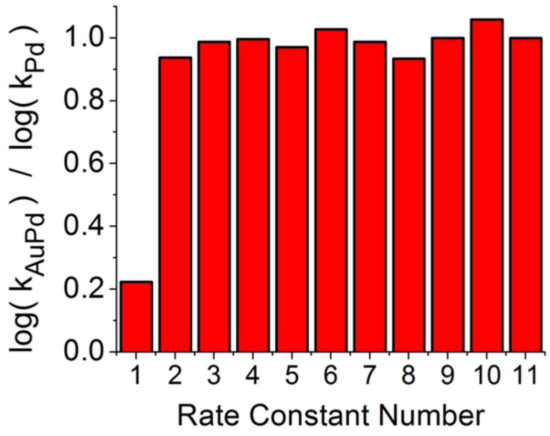

Figure 4: Ratios of the logs of the rate constants between AuPd/C and Pd/C, where the largest change on this scale was in k1.

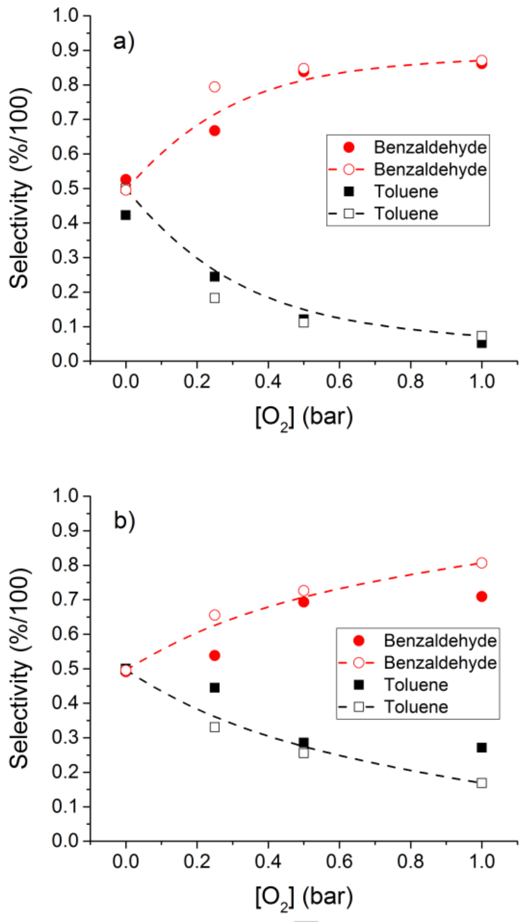

Figure 5: Oxygen dependence of the selectivities towards toluene and aldehyde over for the same reaction conditions as Table 2. Figure a is for Pd and Figure b is for AuPd. Solid symbols are from experiment, while open symbols are from microkinetic modeling simulations. The dashed lines are guides to the eye.

The binding strength and activation energies for O_2 adsorption to the most stable initial and final states over the most stable alloy were calculated, after calculating the energies of 100 different random configurations of AuPd alloys as well as a number of non-random ordered structures. The lowest energy AuPd alloy in our dataset is a non-ordered (no symmetry) configuration which is shown in figure 6 (more details are provided in the Supporting Information). The results of these calculations are provided in Table 3. Energy profiles and images of the dissociation pathways are depicted in Figure 6 and Figure S2. We see that the oxygen energetics display the expected behavior: the energetics of adsorption on the AuPd alloy has a value between those of Au and Pd, such that the total amount of oxygen binding and activation are both reduced relative to pure Pd, consistent with our experimental results.

As in our previous microkinetic study, we used the initial rate of change of aldehyde production to obtain an apparent activation energy: here we obtained a value of 44.5 kJ/mol (Figure 7) which reflects the activation energy of alcohol absorption, Ea2 – as shown by the previous study and consistent with the literature.

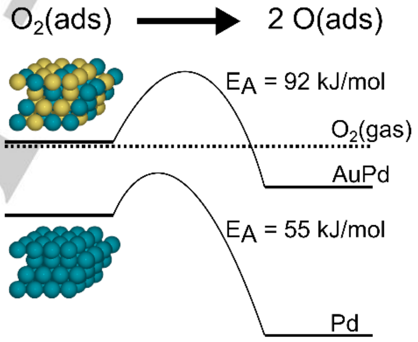

Figure 6: Energy profiles of O_2 dissociation on the AuPd alloy surface and the pure Pd alloy surface, with the gas phase O_2 chemical potential shown for reference.

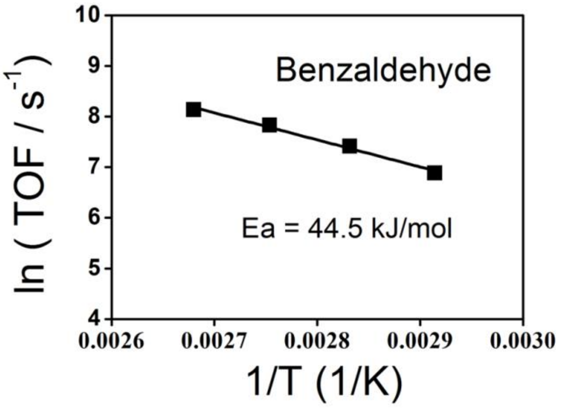

Figure 7: Arrhenius-type plot with the natural log of the early time turnover frequency versus 1/T for benzaldehyde formation. Apparent activation energies were extracted from the slopes.

Plugging in this value of 44.5 kJ/mol for Ea2 into the microkinetic model was able to reproduce most of the temperature dependence observed experimentally, but not the 90-100 °C benzoic acid production and benzene production. The activation energies for the reactions associated with benzoic acid production and benzene production (Ea8 and Ea9) were raised until a good fit was found, with Ea8 = 285 kJ/mol and Ea9=143 kJ/mol. This set of parameters reproduced the trends observed experimentally for all six products, with mostly quantitative agreement (Figure 8).

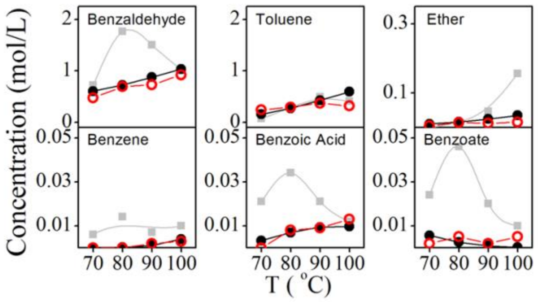

Figure 8: Trends for AuPd/C products temperature dependence. Experimental points: open red circles, Microkinetic model: filled black circles. Experimental data points from Pd/C are shown in gray for comparison.

As noted earlier, we find that the same microkinetic model used for Pd/C in the previous study[6] was able to correctly reproduce all of the trends for AuPd/C and correctly and captures the differences between AuPd/C and Pd/C. For AuPd/C we find that the temperature dependence is mostly governed by the activation energy of k2 (alcohol adsorption), which was also found in the microkinetic modeling of the reaction over Pd/C and is consistent with past literature.[6]

Conclusions

The same micro kinetic model used for Pd/C is able to produce the AuPd/C data. It is expected that AuPd/C would bind oxygen less strongly than Pd/C. Remarkably, almost all of the selectivity changes observed between Pd/C and AuPd/C are explained by a decrease in oxygen adsorption (due to lowering of k1). No excited state electron transfer nor any special local configuration of Au and Pd atoms was required to reproduce the experimental data produced using AuPd.

Acknowledgements

The kinetic simulations and DFT calculations work was supported by the U.S. Department of Energy, Office of Science, Basic Energy Sciences, Chemical Sciences, Geosciences, and Biosciences Division. This research used resources of the Oak Ridge Leadership Computing Facility at the Oak Ridge National Laboratory, which is supported by the Office of Science of the U.S. Department of Energy under Contract No. DE-AC05-00OR22725. TEM works was supported by Karlsruhe Nano Micro Facility (KNMF) long term project.

Keywords: benzyl alcohol • oxidation • gold-palladium • alloy • microkinetic modelling • DFT calculation

[1] a) M. Besson, P. Gallezot, *Catal. Today* **2000**, *57*, 127-141; b) T. Mallat, A. Baiker, *Chem. Rev.* **2004**, *104*, 3037-3058; c) N. Dimitratos, J. A. Lopez-Sanchez, G. J. Hutchings, *Chem. Sci.* **2012**, *3*, 20-44; d) S. E. Davis, M. S. Ide, R. J. Davis, *Green. Chem.* **2013**, *15*, 17-45.

[2] a) J. Luo, H. Yu, H. J. Wang, H. H. Wang, F. Peng, *Chem Eng J* **2014**, *240*, 434-442; b) Y. Yu, B. Lu, X. Wang, J. Zhao, X. Wang, Q. Cai, *Chem Eng J* **2010**, *162*, 738-742.

[3] a) C. Keresszegi, D. Ferri, T. Mallat, A. Baiker, *J. Catal.* **2005**, *234*, 64-75; b) D. Ferri, C. Mondelli, F. Krumeich, A. Baiker, *J Phys Chem B* **2006**, *110*, 22982-22986A; c) M. Sankar, E. Nowicka, P.J. Miedziak, G.L. Brett, R.L. Jenkins, N. Dimitratos, S.H. Taylor, D.W. Knight, D. Bethell, G.J. Hutchings, *Faraday Discuss.* **2010**, *14*5, 341-356; d) A. Savara, C.E. Chan-Thaw, I. Rossetti, A. Villa, L. Prati, *ChemCatChem* **2014**, *6*, 3464 – 3473; e) C. Keresszegi, D. Ferri, T. Mallat, A. Baiker, *J. Phys. Chem. B* **2005**, *109*, 958-967. f) Villa, N. Dimitratos, C. E. Chan-Thaw, C. Hammond, G. M. Veith, D. Wang, M. Manzoli, L. Prati G. J. Hutchings, *Chem. Soc. Rev.*, **2016**, *45*, 4953-4994.

[4] a) F. Gao, D. W. Goodmani, *Chem. Soc. Rev.* **2012**, *41*, 8009-8020; b) A. Villa, D. Wang, D. Su L. Prati, *Catal. Sci. Technol.* **2015**, *5*, 55-68; c) G. Collins, J. D. Holmes, *Adv. Mater.* **2016**, *28*, 5689–5695.

[5] a) M. Chen, D. Kumar, C. W. Yi, D. W. Goodman, *Science* **2005**, *310*, 291-293; b) D. Wang, A. Villa, F. Porta, D. Su, L. Prati, *Chem. Commun*. **2006,** 1956-1958; c) D.I. Enache, J.K. Edwards, P. Landon, B. Solsona-Espriu, A.F. Carley, A.A. Herzing, M. Watanabe, C.J. Kiely, D.W. Knight, G.J. Hutchings, *Science* **2006**, *311*, 362-365; d) W. Hou, N.A. Dehm, R.W.J. Scott, *J. Catal.* **2008**, *253*, 22-27; e) A. Villa, D. Wang, N. Dimitratos, D. Su, V. Trevisan, L. Prati, *Catal. Today* **2010**, *150*, 8-15; f) A. Villa, D. Wang, D. Su, G. Veith, L. Prati, *Phys. Chem. Chem. Phys.*, **2010**, *12*, 2183–2189.

[6] a) A. Savara, I. Rossetti, C. E. Chan-Thaw, L. Prati, A. Villa, *ChemCatChem* **2016**, *8*, 2482 – 2491; b) Savara, A., *Surf. Sci.*, **2016**, *653*, 169-180.

[7] a) A. R. Dento, N. W. Ashcroft, *Phys. ReV. A* **1991**, 3161-3164; b) S.-C.Y. Tsen,; P. A. Crozier, J. Liu, *Ultramicroscopy* **2003**, *98*, 63-72.

[8] A. Villa, D. Ferri, S. Campisi, C. E. Chan-Thaw, Y. Lu, O. Kröcher, L. Prati, *ChemCatChem* **2015**, *7*, 2534 – 2541.

Entry for the Table of Contents (Please choose one layout)

Layout 1:

COMMUNICATION

Microkinetic modelling and density functional theory indicate that changes in the selectivity between Pd/C and AuPd/C in the benzyl alcohol oxidation are explained by a decrease in adsorbed oxygen.

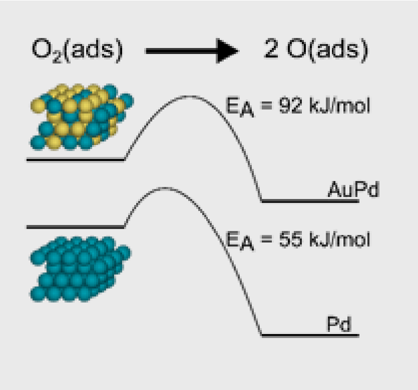

Aditya Savara, Carine E. Chan-Thaw, Jonathan E. Sutton, Di Wang, Laura Prati, and Alberto Villa**

Page No. – Page No.

Title